

Characteristics of the Boundary Layer Structure of Sea Fog on the Coast of Southern China

HUANG Huijun^{1,2} (黄辉军), LIU Hongnian*¹ (刘红年), JIANG Weimei¹ (蒋维楣),
HUANG Jian² (黄健), and MAO Weikang² (毛伟康)

¹*School of Atmospheric Sciences, Nanjing University, Nanjing 210093*

²*Key Open Laboratory for Tropical Monsoon and Joint Open Laboratory of Marine Meteorology,*

Guangzhou Institute of Tropical and Marine Meteorology,

China Meteorological Administration, Guangzhou 510080

(Received 4 November 2010; revised 27 January 2011)

ABSTRACT

Using boundary layer data with regard to sea fog observed at the Science Experiment Base for Marine Meteorology at Bohe, Guangdong Province, the structure of the atmospheric boundary layer and the characteristics of the tops of the fog and the clouds were analyzed. In addition, the effects of advection, radiation, and turbulence during sea fog were also investigated. According to the stability definition of saturated, wet air, the gradient of the potential pseudo-equivalent temperature equal to zero was defined as the thermal turbulence interface. There is evidence to suggest that two layers of turbulence exist in sea fog. Thermal turbulence produced by long-wave radiation is prevalent above the thermal turbulence interface, whereas mechanical turbulence aroused by wind shear is predominant below the interface. The height of the thermal turbulence interface was observed between 180 m and 380 m. Three important factors are closely related to the development of the top of the sea fog: (1) the horizontal advection of the water vapor, (2) the long-wave radiation of the fog top, and (3) the movement of the vertical turbulence. Formation, development, and dissipation are the three possible phases of the evolution of the boundary-layer structure during the sea fog season. In addition, the thermal turbulence interface is the most significant turbulence interface during the formation and development periods; it is maintained after sea fog rises into the stratus layer.

Key words: coast of Southern China, sea fog, boundary layer structure, advection, radiation, turbulence

Citation: Huang, H. J., H. N. Liu, W. M. Jiang, J. Huang, and W. K. Mao, 2011: Characteristics of the boundary layer structure of sea fog on the coast of southern China. *Adv. Atmos. Sci.*, **28**(6), 1377–1389, doi: 10.1007/s00376-011-0191-8.

1. Introduction

Sea fog is water vapor condensation that is observed in the marine boundary layer; it is influenced by processes in the boundary layer such as turbulence exchange, radiation, and entrainment. The various physical mechanisms that have been thought to be responsible for fog formation and its maintenance at sea are the following (Lewis et al., 2004): (1) air brought to saturation by contact with cold sea surface temperatures (SSTs; i.e., advection fog where eddy diffusion is the key mechanism); (2) air brought to saturation

by thermal buoyancy and the resultant lifting; (3) air brought to saturation by radiative cooling in a shallow surface layer, linking maintenance of the fog layer to radiative cooling at the top of the layer; and (4) air brought to saturation by evaporation when cold air streams over water of a much higher temperature.

Advection fog occurs over a large range of locations around the world; it has been shown to occur in the western North Pacific, the North Atlantic, and on the western and eastern coasts of North America, among other locations. The sea fog season on the coast of southern China mainly extends from January to April;

*Corresponding author: LIU Hongnian, liuhn@nju.edu.cn

sea fog in this area is mainly advection fog (Zhang, 1982; Wang, 1983; Zhou and Liu, 1986; Lewis et al., 2004; Gultepe et al., 2007). Research on advection fog indicates a complex relationship between fog formation and the effects of advection, radiation, and turbulence. The development and maintenance of advection fog have different physical mechanisms and processes, indicating that a diversity of the atmospheric and marine conditions exists in the different areas where this type of fog occurs.

In general, advection fog has a close relationship to strong, warm advection, which helps to maintain a surface-based inversion and prevents the warm, moist air mass below the inversion from diffusing into the air above it. These conditions are suitable for continuous cooling by some physical mechanisms, which results in fog formation (Pilié et al., 1979; Wang, 1983). However, a numerical simulation by Hu et al. (2006) demonstrated that turbulence and radiation are the main effects of sea fog formation. In contrast, advection was not shown to have a direct effect on the formation of fog. Taylor (1917) and later Rodhe (1962) established that turbulent heat exchange aroused by wind shear is the key mechanism for the cooling and saturation of the air during the advection process of a warm air mass. Pepper and Lee (1975) showed that the vertical development of advection fog is closely related to the intensity of the wind shear. Hu et al. (2006) have argued that the cooling effect aroused by wind shear turbulence only occurs at the initial phase of fog formation and that it occurs at a low level. The work of Gao et al. (2007) indicates that a thermal internal boundary layer (TIBL) gradually forms at the base of the strong sea surface-based inversion, and that the mechanical turbulence caused by the wind shear results in the moistening of the air and in the transportation of the heat from the air to the sea. Huang et al. (2010b) stated that wind shear turbulence results in (1) a transfer of heat from the air to the SST, (2) a decrease in air temperature, and (3) an increase in air moisture near the sea surface, leading to fog development and maintenance. A great deal of research has been performed concerning the other aspects of fog formation that are affected by radiative cooling. Petterssen (1938) confirmed the role of radiation in the formation and maintenance of sea fog. Lamb (1943) indicated that the loss of heat from the top of the fog results from radiation, which favors fog development. Pilié et al. (1979), Noonkester (1979), Leipper (1994), and Koračin et al. (2001) have indicated that, on the western coast of North America, radiative cooling from the top of the fog plays an important role in fog development through the lowering of stratus clouds. In contrast, Telford and Chai (1984,

1993) reported that radiative cooling from the top of the fog has no effect on fog development. Huang et al. (2010b) reported that heat transfer by radiative cooling from the top of the fog occurs in the same direction as the mechanical turbulence transfer by wind shear, but that it results in fog dissipation by warming the air mass and reducing its moisture level.

More investigation of the atmospheric boundary layer is needed where sea fog occurs to determine the additional effects of advection, radiation, and turbulence. Correlative, notable field programs have been conducted, such as experiments off of the coast of California (CALSPAN) in the 1970s (Pilié et al., 1979), the Cooperative Experiment in West Coast Oceanography and Meteorology in 1976 (CEWCOM'76), and the Project Haar (Findlater et al., 1989). Since 2006, the Guangzhou Institute of Tropical and Marine and Meteorology (ITMM) of the China Meteorological Administration has supported several studies on sea fog using instruments such as tethered balloons. These studies have led to several interesting results, such as the characteristics of the turbulent heat exchange (Qu et al., 2008; Huang et al., 2010b).

From March to April of 2010, the ITMM performed observations again on the atmospheric boundary layer of sea fog at the Science Experiment Base for Marine Meteorology at Bohe, Guangdong Province. In addition, the study used many instruments [e.g., Vaisala global positioning system (GPS) soundings]. The present study mainly investigated the structure of the atmospheric boundary layer and the characteristics of the fog and the cloud tops in the advection fog process. In addition, the effects of advection, radiation, and turbulence on sea fog were also examined. The present paper is organized as follows: section 2 describes the data and the observations. Section 3 describes the main process of the sea fog on 1 and 2 April 2010. Section 4 analyses the characteristics of the boundary layer structure of the sea fog on the coast of southern China. Section 5 presents the main conclusions of the article.

2. Materials

2.1 Site and instruments

The observation site was the same as the one used in 2007 and 2008 (Huang et al., 2009, 2010a), which was located on the Science Experiment Base for Marine Meteorology at Bohe, Guangdong Province (Fig. 1). The Vaisala GPS sounding system, for which the balloon was discharged at a flat 15 m above sea level, and the FM-100 model fog monitor droplet collector (Droplet Measurement Technologies, Inc.), which was located on the observation platform 19 m above sea

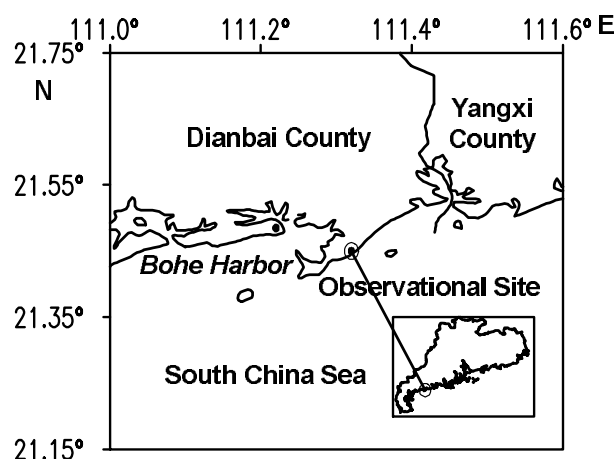


Fig. 1. Observational site location.

level, were used for these experiments.

2.2 The Vaisala GPS sounding data

The air pressure, temperature, relative humidity, wind direction, and wind speed were measured using the GPS sounding system. A total of 55 valid GPS data were collected during the observations of sea fog in 2010, and three relatively intact processes of the sea fog were selected for the present study. Of these three processes, two had relatively short durations of 3–4 h and occurred during the early morning. Only the conditions that occurred on 1 and 2 April quickly developed sea fog that was maintained for a longer period of time. As a result, this more intense sea fog event was selected for atmospheric boundary layer analyses. In addition, two weak sea fog events that occurred on the 5 and 6 April 2010 were also analyzed.

The GPS soundings (2-s intervals, vertical resolution of 4–10 m) related to the more intense sea fog

event were collected from 1800 LST 1 April to 0800 LST 2 April 2010. The exact observation times were as follows: 1800, 2000, and 2200 LST 1 April, and 0000, 0200, 0500, and 0800 LST 2 April. To achieve a series of uniform data, the GPS data were interpolated in the vertical direction with a 10-m interval, and they were also interpolated for time to include the data such as 0400 LST and 0600 LST 2 April. Consequently, eight sets of GPS sounding data (2-h time interval and a 10-m vertical resolution) during the intense sea fog event were used in the analyses. A similar treatment and analysis was also conducted on the weaker sea fog events of 5 and 6 April 2010.

2.3 Other data

The FM-100 model fog monitor droplet collector was used in a manner similar to that of Huang et al. (2010a), and the fog droplet size distribution used in this study included data that were averaged over 1-min intervals. The liquid water content was calculated from the fog droplet size distribution. The atmospheric horizontal visibility data were calculated from the liquid water content in 1-min intervals, using the experience formula that was obtained during by Huang et al. (2009). The calculation of the backward trajectory of airflow used the NCEP/NCAR (National Centers for Environmental Prediction/National Center for Atmospheric Research) reanalysis archive. SSTs were obtained from the NCEP marine modeling and analysis branch operational products.

3. General processes of sea fog

3.1 Synoptic background

The surface weather chart (Fig. 2) shows the period of time during which the sea fog was maintained

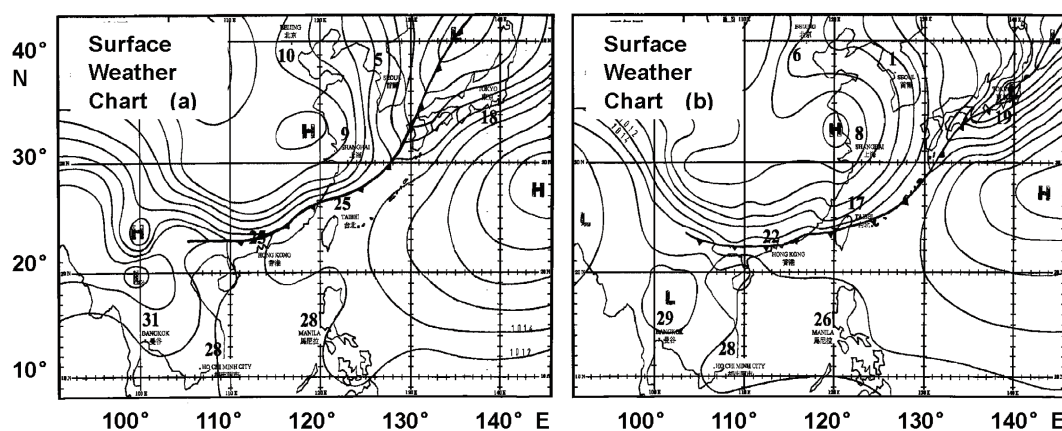


Fig. 2. Surface weather chart (from Hong Kong Observatory). (a) 2000 LST 1 April 2010; (b) 0500 LST 2 April 2010. (Isobaric chart, H is the center of anticyclone, L is the center of cyclone. Temperatures ($^{\circ}$ C) of several main cities are presented.

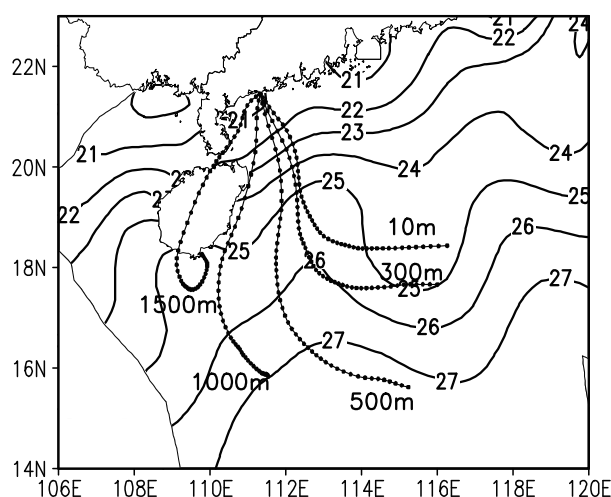


Fig. 3. The distribution of sea surface temperatures (SSTs) and airflow trajectory. The contours denote the daily average of SST ($^{\circ}\text{C}$) on 1 April; the dot-lines denote the 48-h backward trajectory of airflow at 1800 LST 1 April at 10-m, 300-m, 600-m, 1000-m, and 1500-m height.

(from 1800 LST 1 April to 1100 LST 2 April) and the period of time during which the cold front moved away from Lingnan mountain in a southeasterly direction. The southwestern edge of a weak anticyclone on the sea was located on the coast of southern China, in which there was an easterly surface wind. Advection fog forms easily when the warm, moist air mass moves toward the shore across the cold sea surface; the low pressure gradient leads to the formation and maintenance of sea fog. The sea fog dissipated as the cold front passed over the coast. In conclusion, the weather conditions that lead to the formation of sea fog are typical on the coast of southern China (Zhang, 1982).

The distribution of SST and the airflow trajectory (Fig. 3) are represented by the daily average of SST and the 48-h backward trajectory of airflow on 1 April. Figure 3 illustrates that lower air involved in the sea fog event moved from the area north of the South China Sea before its path ended at Bohe. As lower air moved along this trajectory, the underlying ocean temperature changed from $\sim 27^{\circ}\text{C}$ to 21°C .

3.2 Variable characteristics of the basic meteorological elements in low level atmosphere

As shown in Fig. 4a (GPS sounding data), the wind direction was southeasterly near the ground; however, the direction was southwesterly above 1500 m. The wind direction had a clockwise rotation, indicating that the observation station was located near warm advection transport. As shown in Figs. 4b–

d, extreme values of wind speed, temperature, and specific humidity occurred at ~ 100 – 400 m above the ground. These figures show that warm, moist advection transportation occurred ~ 100 – 400 m above the ground during sea fog development (from ~ 0000 to 0500 LST 2 April). According to the graph showing the relative humidity (Fig. 4e), the sea fog was > 600 m above the ground at all times, which indicates that this was a strong sea fog event. The height of the top of the sea fog was changing at all times, a characteristic that will be discussed later in this paper.

As a result of the variability of the surface liquid water content and visibility (Fig. 5), while the warm moist advection transportation strengthened, the surface liquid water content had a sudden, corresponding increase, and the visibility decreased rapidly. When the warm, moist advection transportation weakened between 0500 and 0700 LST, the surface liquid water content rapidly decreased. In addition, visibility increased, showing an inverse relationship with the surface liquid water content. These phenomena indicate that the process of warm, moist advection transportation plays an important role in the variability of the surface liquid water content and visibility in sea fog events.

4. Characteristics of the boundary layer structure of sea fog on the coast of Southern China

4.1 Evolution of the height of the thermal turbulence interface in sea fog

Fog is a condensation phenomenon in the atmospheric boundary layer that occurs when the atmosphere is saturated with moisture. In this saturated, moist atmosphere, the elevated air parcel is subjected to wet adiabatic change. The criterion of stability in the saturated, moist atmosphere has been described as follows: $\partial\theta_{se}/\partial z < 0$ for potential instability (θ_{se} is the potential pseudo-equivalent temperature), $\partial\theta_{se}/\partial z = 0$ for neutral stability, and $\partial\theta_{se}/\partial z > 0$ for potential stability. According to the characteristics of a saturated, moist atmosphere, the height of the potential pseudo-equivalent temperature that equals zero ($\partial\theta_{se}/\partial z = 0$) is defined as the height of the thermal turbulence interface. The potential instability layer exists above the interface, and thermal turbulence develops easily. However, below the interface is the potential stability layer, and thermal turbulence is unlikely to develop. The height of the thermal turbulence interface is between 180 m and 350 m in the process, and its evolution characteristics are shown in Fig. 6. It was observed that when the warm, moist advection transportation strengthened, the height of the thermal

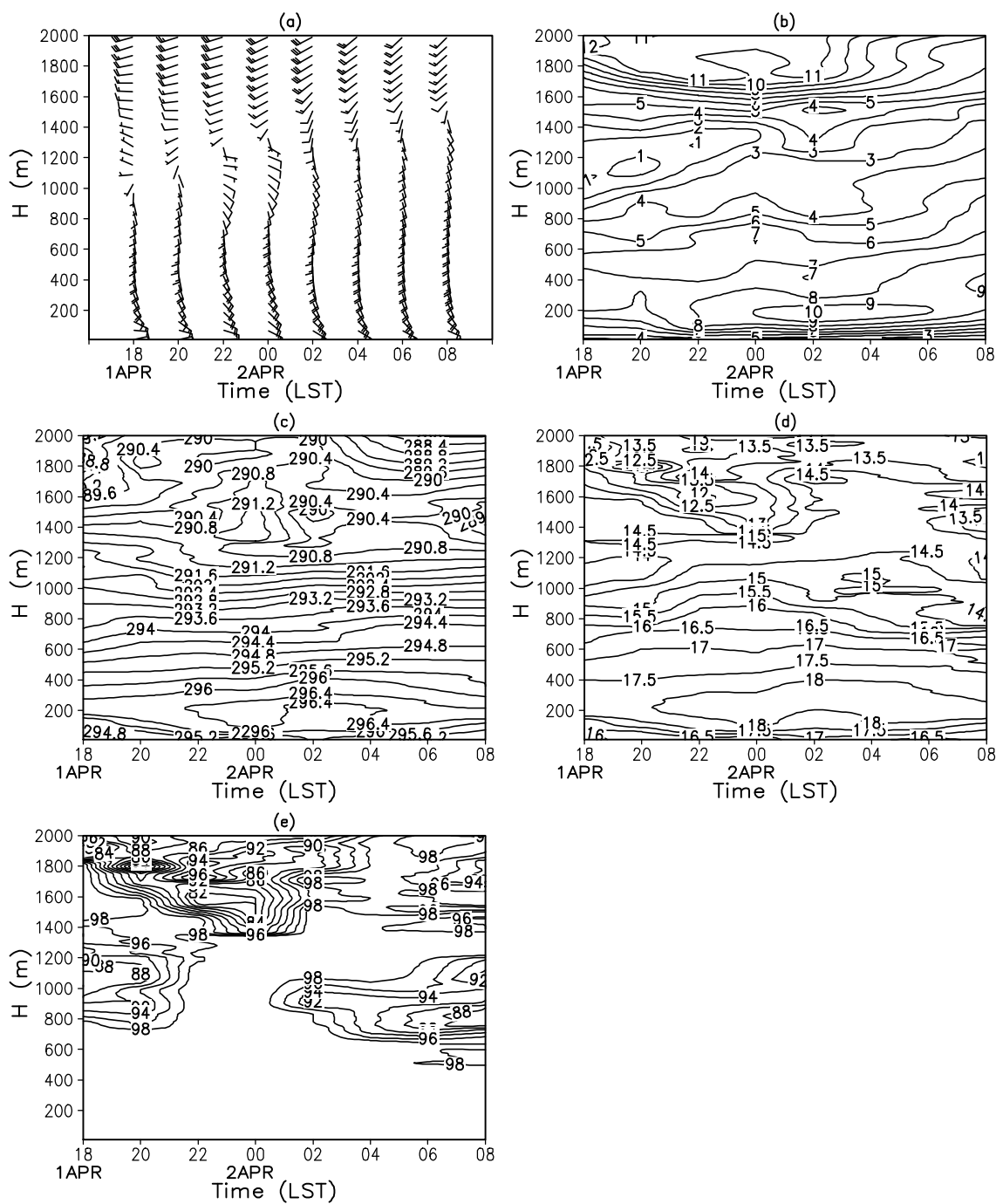


Fig. 4. Variable characteristics of the basic meteorological elements in the lower atmosphere from 1800 LST 1 April to 0800 LST 2 April 2010. (a) wind barb; (b) wind speed (m s^{-1}); (c) temperature (K); (d) specific humidity (g kg^{-1}); (e) relative humidity (%).

turbulence interface correspondingly increased. When the process of the warm, moist advection transportation weakened, the height also decreased. These findings indicate that the warm, moist advection transportation also plays an important role in the height of the thermal turbulence interface of sea fog.

4.2 Characteristics of the basic turbulence structure in sea fog

To investigate the structural characteristics of the meteorological factors below the thermal turbulence interface, we calculated the average value of several of

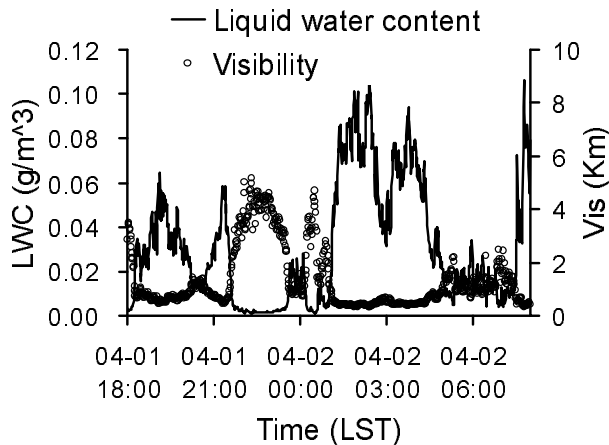


Fig. 5. Variability of the surface liquid water content and visibility on 1 and 2 April 2010.

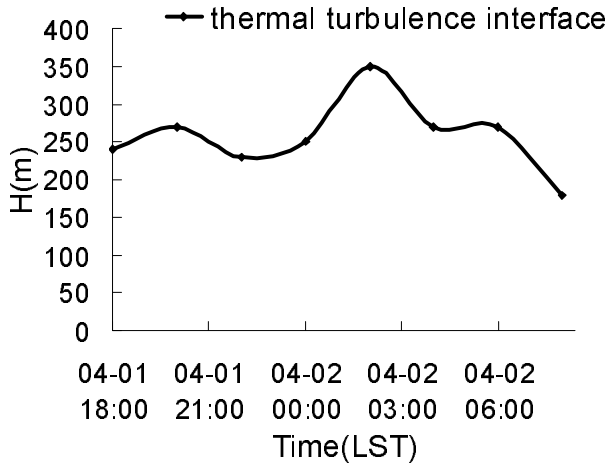


Fig. 6. Evolution of the height of the thermal turbulence interface.

these factors from eight time periods of GPS data (Fig. 7). To find the average, first we interpolated the value of the meteorological factors below the thermal turbulence interface into dimensionless height, with z/h for each time period (z is the real height, h is the height of the thermal turbulence interface), then we averaged the meteorological factors at the same dimensionless height, with z/h from eight time periods of GPS data.

Figure 7 illustrates that, below the thermal turbulence interface, the elevation of the height was accompanied by a gradual elevation in the θ_{se} and q (specific humidity). The wind direction exhibited a gradual transfer from the east near the surface to the south in upper level. The wind speed reached its maximum value below the interface.

The wet Richardson number (Ri_m) was defined as the ratio of the thermal turbulence energy to the me-

chanical turbulence energy in the saturated moist atmosphere; the formula is as follows (Liu et al., 2005):

$$Ri_m = \frac{g}{\theta_{se}} \frac{\partial \theta_{se}}{\partial z} / \left(\frac{\partial \mathbf{V}}{\partial z} \right)^2 \quad (1)$$

Where g is the acceleration due to gravity, and \mathbf{V} is wind vector. Using Eq. (1), we found that two factors are associated with the development of turbulence development. One of these factors is the thermal stability parameter ($1/(\theta_{se})(\partial \theta_{se}/\partial z)$), which indicates that the more unstable the atmospheric stratification, the more likely thermal turbulence is to develop. The other is the vertical wind shear parameter ($\partial \mathbf{V}/\partial z$), which indicates that the stronger the vertical wind shear, the more likely mechanical turbulence is to develop. When $Ri_m = 0$, which indicates that the thermal turbulence energy is equal to zero, the air is in the neutral state. When $Ri_m < 0$ (which indicates that the thermal and mechanical factors are all increasing the likelihood of turbulence), turbulence will definitely develop. When $Ri_m > 0$, the thermal factor results in the weakening of the thermal turbulence; however, the mechanical factor increases the likelihood of mechanical turbulence. According to the Ri_m profile, the Ri_m value is always greater than zero ($Ri_m > 0$) below the thermal turbulence interface, which indicates that the turbulence is mainly produced by the prevalent mechanical factor (Zhao, 2006).

The meteorological element profiles of the lower atmosphere for each time period during the sea fog period are shown in Fig. 8. The Ri_m profiles of each time period (only the values of $-10 \leq Ri_m \leq 10$ are shown) indicate that the wet Richardson number was less than zero ($Ri_m < 0$) beyond the thermal turbulence interface, which indicates that the thermal turbulence predominated above the interface. On the contrary, the wet Richardson number was larger than zero ($Ri_m > 0$) below the interface, which means mechanical turbulence was predominant below the interface.

Similar findings resulted from using the θ_{se} profile in the saturated, moist atmosphere (Fig. 8, the θ_{se} profile in the unsaturated, moist atmosphere is for reference only). Here, $\partial \theta_{se}/\partial z > 0$ below the thermal turbulence interface, indicating that this layer is potentially stable. However, $\partial \theta_{se}/\partial z < 0$ above the interface, indicating potential instability. As a whole, the two atmospheric stratifications in the saturated, moist air of sea fog had different properties, namely potential stability and instability.

In addition, there were different θ_{se} profiles between the sea fog above the thermal turbulence interface and the clouds below the cloud boundary layer. The value of θ_{se} is approximately constant for the clouds below the cloud boundary layer (Deardorff,

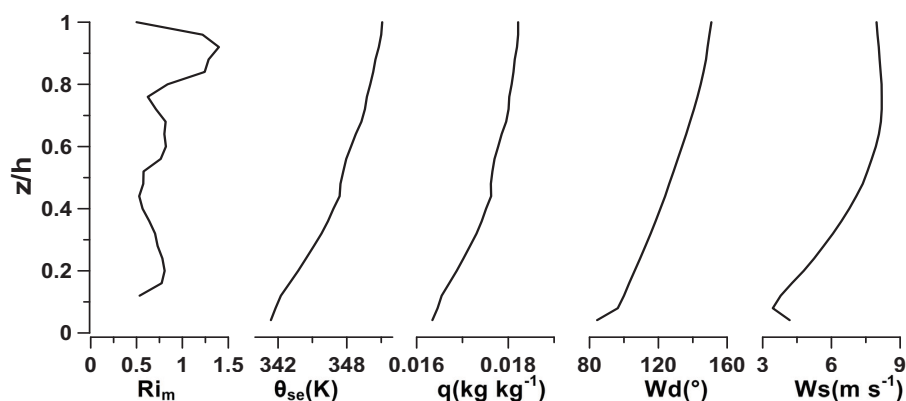


Fig. 7. Averaged profiles of the meteorological factors below the thermal turbulence interface in the sea fog. Ri_m = wet Richardson number, θ_{se} = potential pseudo-equivalent temperature, q = specific humidity, Wd = wind direction, Ws = wind speed.

1980; Stage and Businger, 1981; Stull, 1988). Nevertheless, the value of θ_{se} mainly decreases with the height above the interface in the sea fog, indicating that this layer is potentially unstable.

4.3 Evolution characteristics of the tops of the fog and the clouds during sea fog

According to the observation data at all time points, the tops of the fog and the clouds appeared to change. In this study, the evolution of characteristics of the tops of fog and clouds during selected sea fog events were analyzed in combination with the variable characteristics of the meteorological elements of each time period. [The surface sea fog dissipated to mist when the relative humidity was $< 98\%$ ($RH < 98\%$) during the observation period; therefore, we defined the relative humidity as equal to 98% ($RH = 98\%$) for the top (or base) of the sea fog and clouds in Fig. 8.]

At 1800 LST 1 April, sea fog formed (Fig. 8a). Opaque stratocumulus (Sc OP) and fog were present in the lower atmosphere at the same time and were separated from one another. The wind direction was southeasterly in the fog, whereas the wind direction was southwesterly in the stratocumulus (Sc), indicating that different sources of water vapor transportation were present in the fog and in the Sc.

At 2000 LST 1 April (Fig. 8b), the Sc OP gradually dissipated. The height of the top of the fog was lower than in the former time point, but the mixing movements were more uniform in the fog, and the value of θ_{se} was approximately constant.

From 2000 to 2200 LST, the sea fog rapidly developed (Fig. 8c). When the warm, moist advection transportation became stronger, the thermal turbulence produced by the long-wave radiation at the top of the fog resulted in the rapid upward development of sea fog. The height of the fog top increased from 730 m

to 1180 m. At the fog top during this time period, an evident inversion and a significant change in the wind direction occurred. At the same time, the wind speed reached its minimum value and rapidly increased. In addition, the relative humidity at the top of the fog rapidly decreased.

At 0000 LST 2 April, the fog top height increased to 1340 m (Fig. 8d). The height of the fog top was higher than the base of the inversion, indicating that the sea fog developed rapidly. In the fog layer from the fog top to 200 m below the top, the effect of the long-wave radiation of the fog top and the entrainment process resulted in the value of θ_{se} becoming nearly constant and in very little change in the wind direction. In contrast, the value of θ_{se} decreased below this fog layer. A possible reason for this phenomenon is that, although the sea fog developed rapidly upward, the turbulence mixing was not strong enough to support the development of the fog layer; therefore, vertical mixing was insufficient throughout the fog layer. However, the turbulence mixing still led to a slight change of the wind direction and wind speed in the sea fog.

At 0200 LST 2 April (Fig. 8e), although the sea fog developed continually and reached a height of 1530 m, the amount of the water vapor was insufficient to maintain the saturated status in the fog layer, and dry air entered the sea fog layer as a result of atmospheric entrainment, resulting in a relatively dry layer (between 850 m and 1060 m) in the fog. The sea fog evolved into two layers at this time: the upper layer turned into a stratus (St) layer, and the value of θ_{se} for this stratus layer became nearly constant as a result of the thorough turbulence mixing.

At 0400 LST (Fig. 8f), a large, relatively dry layer (between 670 m and 1030 m) occurred, indicating that the water vapor transported by advection was gradu-

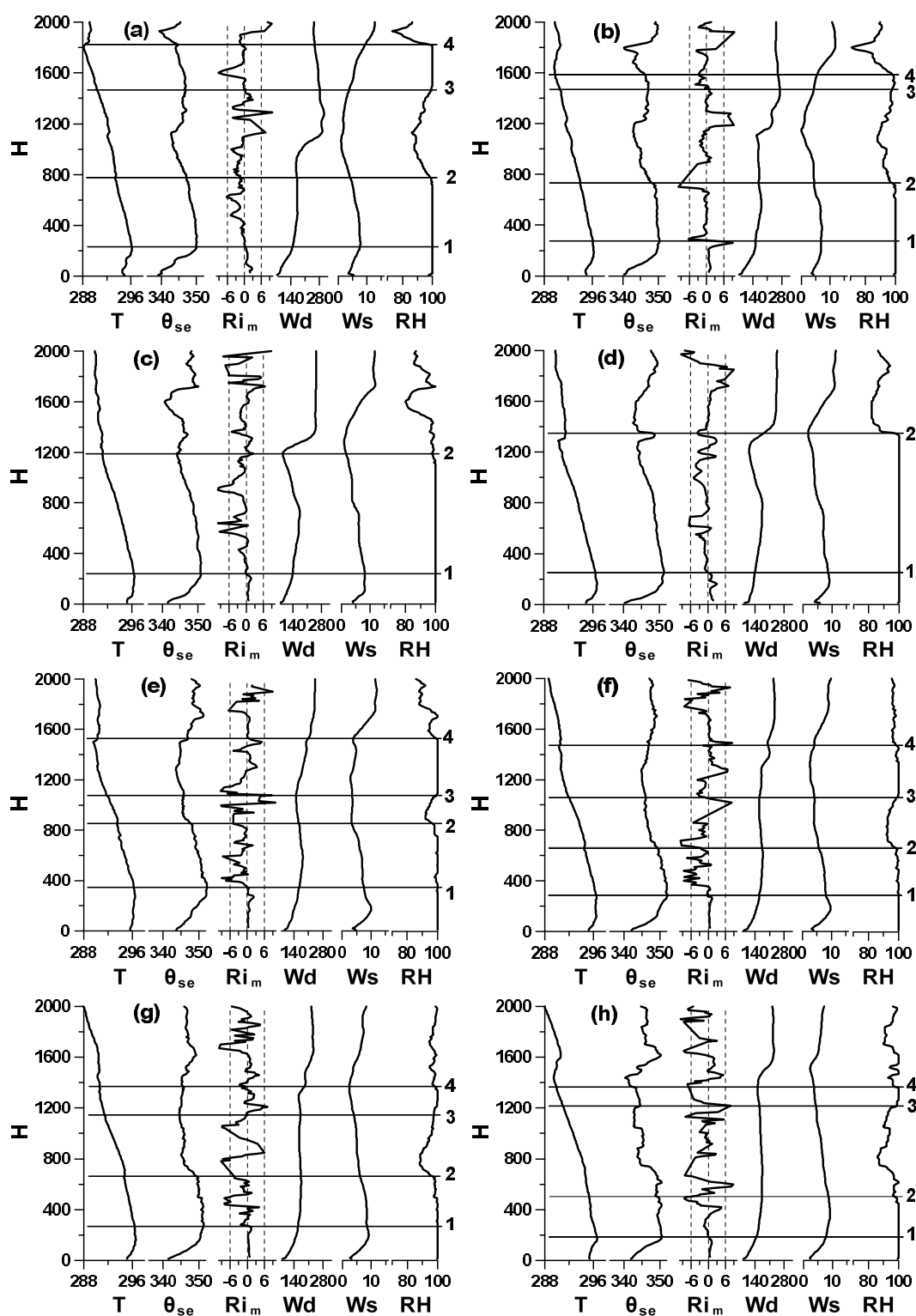


Fig. 8. Meteorological element profiles of the low level atmosphere during sea fog on 1 and 2 April 2010. (1) Height of thermal turbulence interface, (2) top of the fog, (3) base of the cloud, (4) top of the cloud. T =temperature (K), θ_{se} = potential pseudo-equivalent temperature (K), Ri_m = wet Richardson number, Wd = wind direction ($^{\circ}$), Ws =wind speed ($m\ s^{-1}$), RH =relative humidity (%), H = height (m). (a) 1800 LST 1 April; (b) 2000 LST 1 April; (c) 2200 LST 1 April; (d) 2400 LST 2 April; (e) 0200 LST 2 April; (f) 0400 LST 2 April; (g) 0600 LST 2 April; (h) 0800 LST 2 April.

ally decreasing. Both the upper stratus and the nether fog were weakening during this time. This trend continued at 0600 LST (Fig. 8g); the thickness of the upper stratus was thinning; and the nether fog top was falling. Above the fog top, an isothermal layer was present, and the value of θ_{se} decreased in the vertical upward direction. At 0800 LST (Fig. 8h), the amount of water vapor transported by advection was continually decreasing; the upper stratus gradually dissipated; and the nether fog top continued to fall. Notably, the turbulence mixing was still acting in the sea fog; therefore, the wind direction became uniform and the wind speed changed very little in the vertical direction at 0800 LST.

These phenomena allow us to make several conclusions. First, the emergence of sea fog is always accompanied by low clouds on the coast of southern China. Furthermore, low clouds (like stratus) can be formed by a division of layers in the sea fog. In addition, there is a close relationship between the tops of the fog and clouds and the inversion layer. This inversion layer (or isothermal layer) usually corresponds to the tops of the fog and the clouds. Second, two-layer turbulence is a structural characteristic of sea fog. These two layers are composed of the thermal turbulence produced by long-wave radiation above the thermal turbulence interface and the mechanical turbulence caused by the wind shear below the interface. Third, three important factors have a close relationship with the development of the sea fog top on the coast of Southern China: the horizontal advection of the water vapor, the long-wave radiation of the fog top, and the vertical turbulence mixing. As a result of long-wave radiation and the ample transportation of water vapor, fog develops rapidly in the upward direction. Conversely, if the increase in the elevation of the fog top is too rapid, or if the amount of the transportation of the water vapor decreases, the fog layer is divided by the turbulence

and entrainment, resulting in a decrease of the height of the fog top.

4.4 Characteristics of the boundary layer structure of other weak processes of sea fog

Two weak process of sea fog occurred at dawn on 5 and 6 April 2010. The variability of the surface liquid water content and visibility over these two days (Fig. 9) resulted in a duration of the sea fog from 0600 to 1100 LST 5 April, and a duration from 0600 to 0800 LST 6 April. The peak values of the surface liquid water content of the two weak processes of the sea fog events were smaller than those of the former, stronger events of 1 and 2 April. After the dissipation of the sea fog on the ground, the surface visibility increased as a result of the mist condition; the sea fog rose into the stratus; and the base of the cloud remained $\sim 20\text{--}50$ m from the ground.

To analyze the characteristics of the boundary layer structure of weaker sea fog events, the 0800 time points on 5 and 6 April were selected to represent the characteristics of the boundary layer structure during the presence of the sea fog (Figs. 10a and c), and the time points of 1200 LST 5 April and 1100 LST 6 April were selected to represent the characteristics of the sea fog elevation into the stratus (Figs. 10b and d). Figures 10a and c show that, during the weak sea fog event, the profiles of the meteorological elements in the boundary layer were similar to those of the strong sea fog event. The heights of the thermal turbulence interface at 0800 LST 5 and 6 April were 380 m and 300 m, respectively. For the former process, the observed height of the thermal turbulence interface was between 180 m and 380 m. Figures 10b and d show that, when the surface sea fog dissipated into the mist and the sea fog elevated into the stratus, the height of the thermal turbulence interface depicted a stable

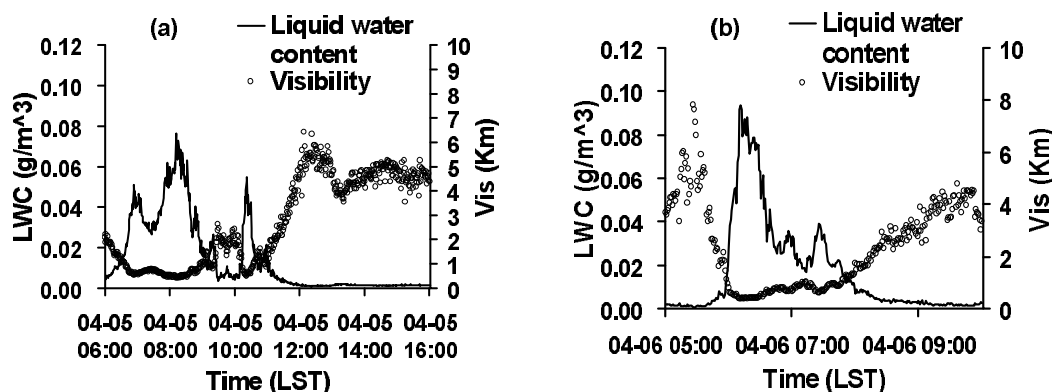


Fig. 9. Variability of the surface liquid water content and the visibility on (a) 5 April and (b) 6 April.

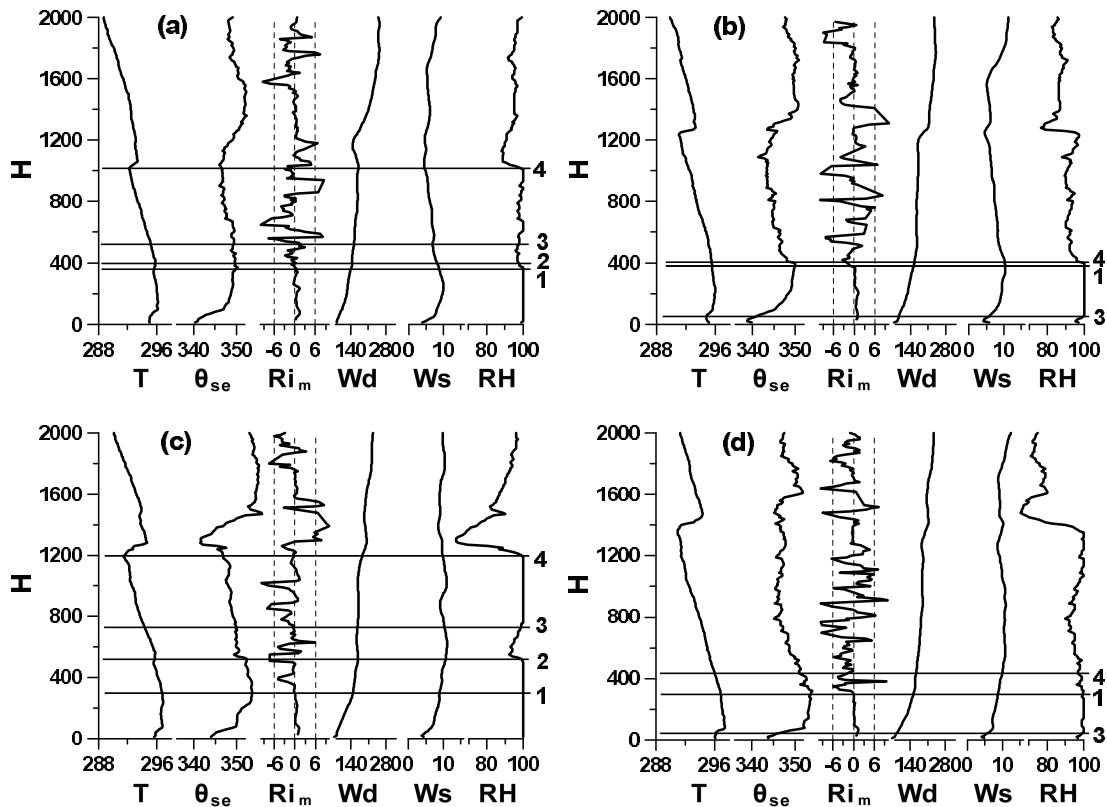


Fig. 10. Meteorological element profiles of the low level atmosphere during sea fog on 5 and 6 April 2010. (a) 0800 LST 5 April; (b) 1200 LST 5 April; (c) 0800 LST 6 April; (d) 1100 LST 6 April.

stratification status of the cloud boundary layer. At this point, the sea fog dissipated as a result of the thermal turbulence and the dry air entrainment above the thermal turbulence interface, and the top of the stratus was slightly higher than the height of the interface commonly. However, the potential stability was maintained in the saturated moist air below the interface. Under the influence of the rise in the SSTs near the coast, the sea fog near the sea surface was elevated into the stratus layer.

Similar characteristics about the thermal turbulence interface existed at the other time points when the sea fog was elevated into the stratus layer. Furthermore, there were no characteristics of the top of the stratus that were lower than the thermal turbulence interface (figures omitted). The height of the thermal turbulence interface depicts the basic characteristic of the stable stratification of the low-level atmosphere before and after sea fog.

4.5 Evolution characteristics of the boundary layer structure of sea fog

As a result of the analysis of the characteristics of the boundary layer structure during weak and strong

sea fog events, we have come to several conclusions concerning the evolution characteristics of the boundary layer structure during sea fog season on the coast of Southern China. The main three possible phases are as follows (Fig. 11).

The first phase is the formation of the sea fog (Fig. 11a). As a result of the transportation of the strong, warm, moist advection, an inversion formed near the sea surface. Next, the stratus formed along with the formation of the thermal turbulence interface. Accompanied by an increase in the air temperature and an accumulation of water vapor near the thermal turbulence interface, the structure of the potential instability strengthened above the interface and combined with the cooling of the long-wave radiation of the fog top. The sea fog continuously developed upward because of the resulting thermal turbulence. In contrast, the structure of the potential stability also strengthened below the interface; the sea fog developed toward the sea surface because of the mechanical turbulence produced by the wind shear and because of a cooling effect by the sea surface. As a result, the sea fog formed.

The second phase is the development of the sea

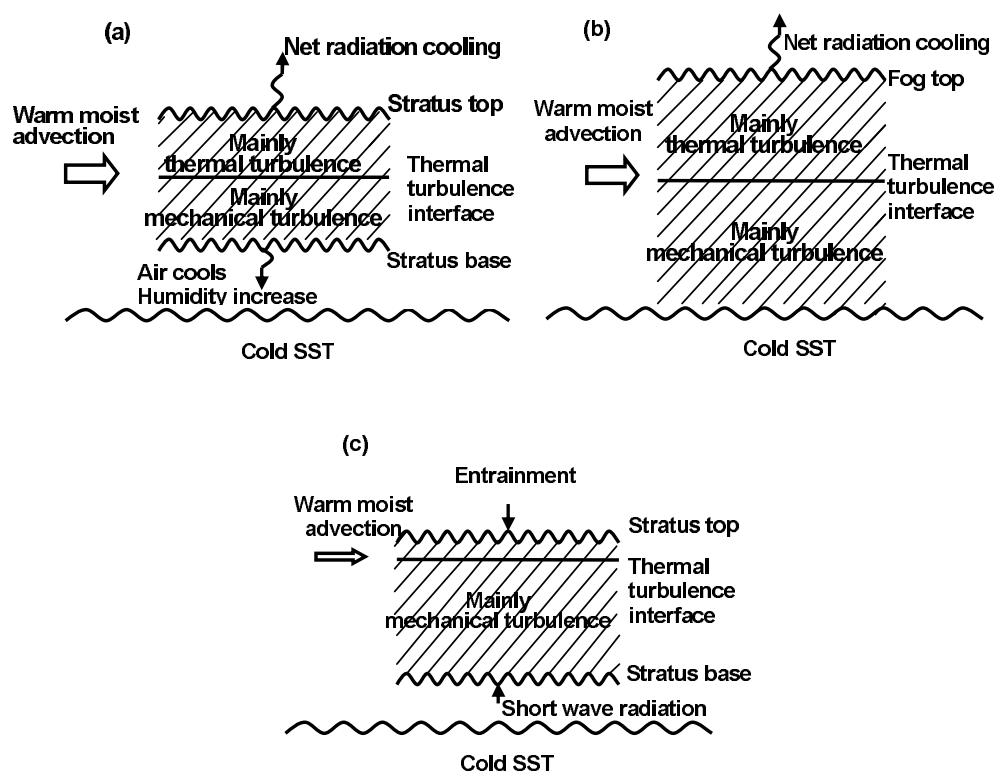


Fig. 11. Evolution characteristics of the boundary layer structure of sea fog. (a) Phase 1: formation; (b) Phase 2: development; (c) Phase 3: dissipation.

fog (Fig. 11b). The strong, warm, moist advection transported continuously during this phase. Above the interface, the sea fog grew upward as a result of the thermal turbulence, and the fog top grew higher and higher. At this point in time, if the height of the fog top elevated too quickly, the sea fog layer might be split by the entrainment, due to the shortage of the total water vapor transported by the warm moist advection. Below the interface, the saturated warm moist air was also transported toward the sea surface as a result of the mechanical turbulence produced by the wind shear, causing the sea fog near the sea surface to be thicker and causing visibility to decrease.

The third phase is the dissipation of the sea fog (Fig. 11c). As a result of the weakening of the transportation of the warm, moist advection, the sea fog gradually elevated into the stratus. Above the interface, as a result of the shortage of water vapor, the sea fog slowly dissipated with the help of the turbulence and entrainment, and the stratus top was a little higher than the height of the interface. Below the interface, as a result of the short-wave radiation, the SSTs increased near the coast, and the sea fog rose into the stratus. Notably, during sea fog season, especially between two sea fog events, the boundary layer structure with the stratus layer above the ground often ex-

isted. Because of the weak, warm, moist advection, the thermal turbulence interface was maintained. At the same time, the saturated moist air below the interface had potential stability; therefore, the stratus layer also remained. When some favorable meteorological conditions in existence (such as the occurrence of a strong warm moist advection or a decrease in the coastland air temperature near the sea surface at dawn), the sea fog will develop base on the stratus layer. This phenomenon has been observed in many sea fog processes.

In view of the present analysis, the thermal turbulence interface has been shown to play an important role in the three possible phases of the evolution of the boundary layer structure in the sea fog season of the coast of southern China. This interface is significant during the formation and development of sea fog. In addition, after sea fog has been elevated into the stratus layer, this interface is the factor that maintains the layer.

5. Conclusion

The boundary layer observation data during sea fog events were collected at the Science Experiment Base for Marine Meteorology at Bohe, Guangdong Province. First, the structure of the atmospheric

boundary layer in advection fog was investigated. Second, the variable characteristics of the fog and cloud top were analyzed, along with the effects of advection, radiation, and turbulence during sea fog. Third, the significance of the thermal turbulence interface was revealed, and the three possible phases of the evolution process of the boundary layer structure of sea fog were also discussed. The main results are as follows:

(1) According to the stability definition of saturated wet air, two properties of atmospheric stratification, potential stability and potential instability, have been revealed in the saturated wet air of sea fog. Consequently, the gradient of the potential pseudo-equivalent temperature was equal to zero ($\partial\theta_{se}/\partial z = 0$) and was defined as the thermal turbulence interface.

(2) During the advection fog period, a warm, moist advection process existed at a height between 100 m and 400 m. As the warm, moist advection process was enhanced or weakened, two aspects were influenced: one aspect was the magnitude of the liquid water content in the sea fog near the surface. When the advection process was enhanced, the surface liquid water content increased and the visibility decreased. In contrast, when the advection process weakened, the surface liquid water content decreased and visibility increased. Another aspect was the height of the thermal turbulence interface in the sea fog. When the advection process was enhanced, the height of the thermal turbulence interface increased; it decreased if the advection process weakened.

(3) On the coast of southern China, the emergence of sea fog was always accompanied by a low cloud layer. Furthermore, sometimes the formation of this low cloud layer was a result of the layered division of the sea fog into two parts. In addition, a close relationship exists between the tops of the fog and the clouds and the inversion layer: The inversion layer (or the isothermal layer) usually corresponds to the tops of the fog and the clouds.

(4) Two layers of turbulence were shown to exist in the sea fog. The thermal turbulence produced by the long-wave radiation was prevalent above the thermal turbulence interface, and the mechanical turbulence aroused by the wind shear was predominant below the interface. The height of the thermal turbulence interface was observed between 180 m and 380 m.

(5) Three important factors have a close relationship with the development of the sea fog top on the coast of southern China: the horizontal advection of the water vapor, the long-wave radiation of the fog top, and the vertical turbulence mixing. As a result of long-wave radiation and the ample transportation of water vapor, fog developed in the upward direction. However, if the elevation of the fog top increased

too quickly or if the transportation of water vapor decreased, the fog layer was divided by the turbulence and entrainment, resulting in a decrease in the height of the fog top.

(6) Formation, development, and dissipation are the three possible phases of the evolution of the boundary layer structure during sea fog events on the coast of southern China. The thermal turbulence interface was shown to play an important role in these phases. The interface is significant during the formation and the development of sea fog. Also, after sea fog has been elevated into the stratus layer, this interface is the main factor that maintains the layer.

In this study, the structure of the atmospheric boundary layer in advection fog was studied, and the importance of the thermal turbulence interface was revealed. In addition, the effects of advection, radiation, and turbulence during sea fog have also been discussed, as has the relationship between the sea fog and the stratus. However, these results need to be confirmed using a dynamical model that adequately accounts for the processes of turbulence and radiation and the interaction between the sea fog and the stratus. This will be the next step in our continuing research.

Acknowledgements. This research was sponsored jointly by the Chinese Special Scientific Research Project for Public Interest (Grant No. GYHY200906008), the National Natural Science Foundation of China (Grant No. 40675013), the Science and Technology Project of Guangdong Province (Grant No. 2008B030303072), and the Meteorological Sciences Research Project of the Weather Bureau of Guangdong Province (Grant No. 201003). The authors wish to thank two reviewers, especially J. M. Lewis and his colleague. They carefully reviewed the manuscript and made many constructive suggestions. Special thanks to the staff at the Science Experiment Base for Marine Meteorology at Bohe, Guangdong Province, and to the weather bureau of Maoming.

REFERENCES

- Deardorff, J. W., 1980: Cloud top entrainment instability. *J. Atmos. Sci.*, **37**, 131–147.
- Findlater, J., W. Roach, and B. McHugh, 1989: The haar of north-east Scotland. *Quart. J. Roy. Meteor. Soc.*, **115**, 581–608.
- Gao, S. H., H. Lin, B. Shen, and G. Fu, 2007: A heavy sea fog event over the Yellow Sea in March 2005: analysis and numerical modeling. *Adv. Atmos. Sci.*, **24**, 65–81, doi: 10.1007/s00376-007-0065-2.
- Gultepe, I., and Coauthors, 2007: Fog research: A review of past achievements and future perspectives. *Pure Appl. Geophys.*, **164**, 1121–1159.
- Hu, R. J., K. H. Dong, and F. X. Zhou, 2006: Numerical

- experiments with the advection, turbulence and radiation effect in the sea fog formation process. *Adv. Marine Sci.*, **24**(2), 156–165. (in Chinese)
- Huang, H. J., J. Huang, C. X. Liu, J. N. Yuan, W. H. Lü, Y. Q. Yang, W. K. Mao, and F. Liao, 2009: Microphysical characteristics of the sea fog in Maoming area. *Acta Oceanologica Sinica*, **31**(2), 17–23. (in Chinese)
- Huang, H. J., J. Huang, W. K. Mao, F. Liao, X. N. Li, W. H. Lü, and Y. Q. Yang, 2010a: Characteristics of liquid water content of sea fog in Maoming area and its relationship with atmospheric horizontal visibility. *Acta Oceanologica Sinica*, **32**(2), 40–53. (in Chinese)
- Huang, J., and Coauthors, 2010b: Turbulence heat exchange in a warm sea fog event on the coast of the South China. *Chinese J. Atmos. Sci.*, **34**(4), 715–725. (in Chinese)
- Koraćin, D., J. Lewis, W. T. Thompson, C. E. Dorman, and J. A. Businger, 2001: Transition of stratus into fog along the California coast: Observations and modeling. *J. Atmos. Sci.*, **58**, 1714–1731.
- Lamb, H., 1943: Haars or North Sea fogs on the coasts of Great Britain. Meteorology Office Publication M. O. 504, 24pp.
- Leipper, D. F., 1994: Fog on the United States west coast: A review. *Bull. Amer. Meteor. Soc.*, **75**, 229–240.
- Lewis, J. M., D. Koraćin, and K. T. Redmond, 2004: Sea fog research in the United Kingdom and United States: A historical essay including outlook. *Bull. Amer. Meteor. Soc.*, **85**, 395–408.
- Liu, J. W., H. Guo, Y. D. Li, H. Z. Liu, and B. J. Wu, 2005: *Calculational Basic for Parameters of Synoptic Analysis and Forecast*. China Meteorological Press, Beijing, 117–122. (in Chinese)
- Noonkester, V. R., 1979: Coastal marine fog in Southern California. *Mon. Wea. Rev.*, **107**, 830–851.
- Pepper, D. W., and S. C. Lee, 1975: Transport phenomena in thermally stratified boundary layers. *Journal of Heat Transfer*, **2**, 60–65.
- Petterssen, S., 1938: On the causes and the forecasting of the California fog. *Bull. Amer. Meteor. Soc.*, **19**, 49–55.
- Pilić, R. J., E. J. Mack, C. W. Rogers, U. Katz, and W. C. Kocmond, 1979: The formation of marine fog and the development of fog-Stratus Systems along the California coast. *J. Appl. Meteor.*, **18**, 1275–1286.
- Qu, F. Q., S. D. Liu, Y. M. Yi, and J. Huang, 2008: The observation and analysis of a sea fog event in South China Sea. *Journal of Tropical Meteorology*, **24**(5), 490–496. (in Chinese)
- Rodhe, B., 1962: The effect of turbulence on fog formation. *Tellus*, **14**, 49–86.
- Stage, S. A., and J. A. Businger, 1981: A model for entrainment into a cloud-topped marine boundary layer. Part I: model description and application to a cold-air outbreak episode. *J. Atmos. Sci.*, **38**, 2213–2229.
- Stull, R. B., 1988: *An Introduction to Boundary Layer Meteorology*. Kluwer Academic Publishers, 670pp.
- Taylor, G. I., 1917: The formation of fog and mist. *Quart. J. Roy. Meteor. Soc.*, **43**, 241–268.
- Telford, J. W., and S. K. Chai, 1984: Inversions and fog, stratus and cumulus formation in warm air over cooler water. *Bound.-Layer Meteor.*, **29**, 109–137.
- Telford, J. W., and S. K. Chai, 1993: Marine fog and its dissipation over warm water. *J. Atmo. Sci.*, **50**, 3336–3349.
- Wang, B. H., 1983: *Sea Fog*. China Ocean Press, Beijing, 358pp. (in Chinese)
- Zhang, F. C., 1982: Statistical analysis of sea fog in the Northwest Pacific Ocean. *Acta Oceanologica Sinica*, **4**(2), 157–168. (in Chinese)
- Zhao, M., 2006: *Dynamics of Atmospheric Boundary Layer*. Higher Education Press, Beijing, 350pp. (in Chinese)
- Zhou, F. X., and L. T. Liu, 1986: Sea fog. *Acta Shandong Institute of Oceanography*, **16**(1), 114–131. (in Chinese)